Received: 13 July 2023 | Revised: 5 December 2023 | Accepted: 14 December 2023

DOI: 10.1111/1750-3841.16911

Journal of Food Science WILEY

ORIGINAL ARTICLE

Food Engineering, Materials Science, and Nanotechnology

Characterization of fruit pulp-soy protein isolate (SPI) complexes: Effect of superfine grinding

Jin Xie[1,2] | **Jian Lyu**[1] | **Fengzhao Wang**[1] | **Lansha Bai**[1] | **Jinfeng Bi**[1]

[1]Institute of Food Science and Technology, Chinese Academy of Agricultural Sciences, Key Laboratory of Agro-products Processing, Ministry of Agriculture and Rural Affairs, Beijing, China

[2]Gembloux Agro-Bio Tech, Unit of Food Science and Formulation, University of Liège, Gembloux, Belgium

Correspondence
Jinfeng Bi and Jian Lyu, Institute of Food Science and Technology, Chinese Academy of Agricultural Sciences, Key Laboratory of Agro-products Processing, Ministry of Agriculture and Rural Affairs, Beijing 100193, China.
Email: bjfcaas@126.com and lvjianlinjian@163.com

Funding information
Agricultural Science and Technology Innovation Program of Institute of Food Science and Technology, Chinese Academy of Agricultural Sciences (CAAS-ASTIP-Q2022-IFST-15); China Agriculture Research System of MOF and MARA, Grant/Award Number: (CARS-30-5-02)

Abstract: Superfine grinding (SG), as an innovative technology, was conducted to improve the physicochemical and structural properties of fruit pulps. Nectarine, apple, and honey peach were selected as the materials. With the increase in SG frequency, the soluble solids content, viscosity, $D[4, 3]$, $D[3, 2]$, G' and G'' of fruit pulps were evidently decreased, whereas the turbidity was increased. The smallest $D[4, 3]$ (294.90 μm) and $D[3, 2]$ (159.67 μm) were observed in nectarine pulp under SG at 50 Hz. The highest turbidity (266.33) was shown in honey peach pulp under SG at 50 Hz. The active groups of the fruit pulps with SG were exposed by Fourier transform infrared spectroscopy (FT-IR). Notably, the excessive destruction in structure was confirmed in SG with 50 Hz. With soy protein isolate (SPI) addition, $D[4, 3]$ and $D[3, 2]$ of complexes decreased, whereas G' and G'' increased. The formation of new fruit pulp-SPI complexes was demonstrated by FT-IR and LF-NMR analysis. The dense and uniform structure was found in complexes prepared by SPI and fruit pulp with 30 Hz SG. Especially, apple-SPI complex with 30 Hz SG showed the highest water-holding capacity (WHC) (0.75) and adhesiveness (7973.00 g s). A significant correlation between fruit pulps and the complexes was revealed. Taken together, the impact of SG modification on fruit pulps would enhance WHC, rheology, and textural properties of the fruit pulp-SPI complexes, especially for SG with 30 Hz.

KEYWORDS
electrostatic interaction, peach pulp, soy protein isolate, superfine grinding, texture

Practical Application: This research provided a comprehensive exploration of the potential of SG technology to modify fruit pulps, solving the diversity of textural customization problems and offering valuable insights for the development of semisolid food products.

1 | INTRODUCTION

With the trend of population aging, the elderly suffering from chewing and swallowing problems are increasing rapidly. The elderly often experience tooth loss, decreased oral or tongue muscle strength, and weakness of other physiological functions (Laguna et al., 2016). To cater to the needs of the elderly with dysphagia, semisolid foods with gel-like properties produced by proteins or polysaccharides have been given more prominence. These foods minimize the effort required for mastication and oral processing (Godoi et al., 2017). For further improving the

physicochemical properties of semisolids, polysaccharides were extensively applied to the protein matrix, which could enhance the water binding capacity, stabilize the structure, produce stable foam, and promote uniformity (Varela et al., 2014). This phenomenon might be attributed to the gelling capacity of polysaccharides, which would accelerate the cross-link action with proteins. Additionally, the nonthermal processing, for example, ultrasound and homogenization, could promote structure exposure alongside the denaturation of protein, which might facilitate the aggregation behavior of protein (Li et al., 2023; Wang et al., 2018). When subjected to the addition of *Mesona blumes* polysaccharide (MBP), the electrostatic and hydrophobic interactions between soy protein isolate (SPI) and MBP were enhanced, which contributed to the formation of three-dimensional structure and the improved water-holding capacity (WHC) and gel strength of the complex (Wang et al., 2020). Similarly, exposed amino acid residue in whey protein isolate was associated with the hydroxyl of κ-carrageenan, resulting in the formation of a dense network along with the high gel strength (fracture stress) and firmness (Çakır & Foegeding, 2011). Considering the promotion effect of polysaccharides on complex systems, it is reasonable to conclude that the dense structure and the functional properties may be owing to the synergistic effect of polysaccharides on protein. Polysaccharides play a crucial role in enhancing the properties of these complex systems.

As the firm texture of fruits that are rich in dietary polysaccharides can pose challenges for the elderly with chewing or swallowing difficulties (Buggenhout et al., 2015), various methods have been developed to alter the natural texture characteristics of fruits to adapt to the elderly needs. Pulping as a traditional alternative texture technology can make the fruit more friendly for the elderly to consume sufficient amounts of fruit polysaccharides. To obtain fruit pulp with excellent physicochemical properties, high-pressure homogenization (HPH) technology has been widely studied (Buggenhout et al., 2015), which could significantly reduce the particle sizes of the plant-based matrix to a micro-scale level. However, HPH technology was limited in the food industry because of the high cost. Alternative methods, including steam explosion and supercritical CO_2 explosion, were used to degrade the cellulose and hemicellulose in fruit pulp, which could promote edibility for the elderly (Moelants et al., 2012). Generally, steam explosion and supercritical CO_2 as the energy-intensive technologies were conducted under high temperature, which led to the significant degradation of heat-sensitive components. Additionally, these technologies usually required specialized equipment and expertise, which limited their application in food industry (Tan & Kerr, 2015). Superfine grinding (SG), known for its powerful shearing and grinding capabilities, is a promising technology for reducing particle size and improving the physicochemical properties of fruit pulp (Huang et al., 2018). When subjected to SG processing, the polysaccharides in ginger powder unfolded to expose more hydrophilic groups and captured the moisture through the hydrogen bond, which reflected in a good WHC, dispersibility, and solubility (Zhao et al., 2009). Furthermore, the small homogeneous particle size and the bright color were observed in sugar beet powder after SG modification. It was speculated that SG would facilitate the internal structure unfolding in cellulose and hemicellulose to expose sufficient active sites to improve the quality (Huang et al., 2018). However, limited research focused on the modification of SG on fruit pulps and semisolids in which fruit pulps were the main matrix.

This study aimed to investigate the effect of SG on the physicochemical and structural properties of different fruit pulps, which were used as the main matrix of the semisolids. In detail, we evaluated the properties of fruit pulps, such as pH, soluble solids content (SSC), water content, turbidity, particle size, rheological behavior, microstructure, and Fourier transform infrared spectroscopy (FT-IR). Then, SPI was added to fruit pulps to prepare the fruit pulp-SPI complexes, respectively. The physicochemical properties, microstructure, texture, and sensory evaluation of fruit pulps-SPI complexes were also investigated. At last, correlation analyses were used to reveal potential relevance between fruit pulp processed by SG and the semisolids consisting of fruit pulp and SPI. In this study, the fruit pulp-SPI complex was developed as semisolid food with appropriate texture characteristics, which might provide a new solution for improving and controlling textural quality for people with dysphagia.

2 | MATERIALS AND METHODS

2.1 | Material

SPI (content ≥90%, analytical grad) was purchased from Shanghai Yuanye Bio-Technology Co., Ltd. Nectarines (*Zhongyoujinhui*), apples (*Fuji*), and honey peaches (*Spring snow*) were purchased from a local Hualian supermarket (Beijing, China) and selected in good condition without deterioration.

2.2 | Preparation of fruit pulps

Nectarines (1.2 kg), apples (1.2 kg), and honey peaches (1.2 kg) were washed, sliced after removing the kernels, and

ground for 2 min using a blender (Supor, Co. Ltd), respectively. Fruit pulps (1 kg) obtained from the previous step were ground by SG equipment (Qingdao UnisonEco Food Technology Co. Ltd) for another 2 min at 30 or 50 Hz in a vacuum condition, respectively. The control ones, namely, nectarine pulp, apple pulp, and honey peach pulp, were named N, A, and H, respectively. The nectarine, apple, and honey peach pulps treated by SG processing at 30 Hz were named 30N, 30A, and 30H, respectively. The nectarine, apple, and honey peach pulps treated by SG at 50 Hz were named 50N, 50A, and 50H, respectively.

2.3 | Preparation of nectarine-SPI, apple-SPI, and honey peach-SPI complexes

The complexes were first prepared by the addition of SPI into fruit pulps, with a weight ratio of 1:9, respectively. Briefly, the fruit pulp-SPI mixer was stirred using a homogenizer (RW 20 digital, IKA) with 560 rpm/min for 2 min and then heated to 80°C in a water bath for 30 min, followed by cooling at room temperature and refrigeration at 4°C overnight to form the complexes. The complexes with N, A, and H were marked as N-SPI, A-SPI, and H-SPI, respectively. The complexes with 30N, 30A, and 30H were marked as 30N-SPI, 30A-SPI, and 30H-SPI, respectively. The complexes with 50N, 50A, and 50 Hz were marked as 50N-SPI, 50A-SPI, and 50H-SPI, respectively.

2.4 | pH soluble solids content (SSC), water content, and turbidity of pulps and complexes

The pH, SSC, and turbidity of pulps and complexes were evaluated by a thermal gravimetric analyzer (TGA 4000, PE Instruments Inc.), Abbe refractometer (MASTER-2α, Hitachi), and turbidimeter (2100N, HACH), respectively. The water content was measured by the direct drying method (AOAC, 2005).

2.5 | Particle size

Particle size distribution was measured by a laser particle size analyzer (S3500, Microtrac) with an aligned detector and laser after calibrating the backgrounds. Before testing, the samples were diluted 10 times with Milli-Q water. Three measurements were conducted for each sample with 15 runs and each run lasted for 10 s. Particle size was displayed in terms of the volume mean diameter $D[4, 3]$ and $D[3, 2]$.

2.6 | Rheological properties

Rheological measurements of complexes were performed with a rheometer (TA Instruments) equipped with the parallel plates geometry (40 mm diameter). The dynamic testing was programmed in frequency sweep according to Liu et al. (2017). Samples (5.0 ± 0.1 g) were added between two parallel plates, and experimental flow curves of pulps and complexes were constructed through continuous shear over a shear rate range of 0.01–100 S^{-1} at 25°C. The frequency-dependent storage modulus (G') and loss modulus (G'') were measured at a constant temperature of 25°C and a fixed strain of 1% followed by frequency sweep tests.

2.7 | Microstructure

All samples were freeze-dried, fixed, and gold sputtering treated and then observed by a scanning electron microscope (SU8010, Hitachi Co.) to obtain their microstructures. The magnification was 250× at an acceleration voltage of 10 kV.

2.8 | Fourier transform infrared spectroscopy (FT-IR)

All samples were freeze-dried and mixed with KBr powder (1:100, w/w) to prepare the pellet to obtain the FT-IR spectra. An FT-IR spectrophotometer (Tensor 27, Bruker) was used with a resolution of 4 cm^{-1}, a cumulative scan of 64, and a wavelength range of 4000–400 cm^{-1} at room temperature.

2.9 | Textural analysis

A texture analyzer (TA-XT2, Stable Micro System Co., Ltd.) with a TA/BE probe and a 35 mm flat compression plate was applied to measure the hardness and adhesiveness of the samples. The compression strain was set to 70%. The pretest, test, and posttest speeds were set to 5, 2, and 2 mm/s, respectively.

2.10 | Water-holding capacity (WHC)

WHC of the samples was determined using the centrifugation procedures according to Munialo et al. (2016). WHC was defined as the percentage of gel weight after centrifugation relative to the gel weight before centrifugation.

Samples (5.0 ± 0.1 g) were placed in the spin tubes and centrifugated at 8000 r/min for 10 min at 4°C. WHC was calculated in the following equation:

$$\mathrm{WHC} = \frac{W_2 - W}{W_1 - W} \quad (1)$$

where W was the weight of the tube, g; W_1 was the initial total weight of samples and tubes, g; and W_2 was the total weight of tubes and samples after centrifugation, g.

2.11 | Water distribution

The transverse relaxation time (T_2) analysis was performed by an LF-NMR analyzer (MiniMR-60, Suzhou Niumag Analytical Instrument Corporation) equipped with 0.5 T permanent magnet corresponding to a proton resonance frequency of 23.2 MHz at 25.00 ± 0.02°C. Parameters for T_2 relaxation time measurements were settled as follows: time waiting = 2000 ms, time echo = 0.5 ms, number of echoes = 12,000, and number of scans = 4. Logarithmic coordinates of raw data were used to construct the T_2 distribution curves with a multi-exponential model under the program of the MultiExp Inv Analysis (Suzhou Niumag Analytical Instrument Corporation) (Wang et al., 2016).

2.12 | Sensory evaluation

The sensory evaluation was conducted by 30 trained food science students (15 females and 15 males, aged varied from 20 to 30 years) in laboratory conditions. The color, flavor, texture, and overall evaluation were selected to evaluate the quality and attractiveness of the complex samples. The sensory evaluation was conducted according to the International Organization for Standardization (ISO) (2016). The sensory analysis was divided into the following categories on a 0–10 hedonic scale. Color: Irregular dark or brown (0), typical apple or peach color (10). Flavor: imperceptible (0), intensive (10). Texture: mobile-like liquid (0), coagulated-like gel (10). Overall evaluation of food quality: poor (0), excellent (10). The samples were coded with two-digit random numbers and evaluated in random order.

2.13 | Statistical analysis

Data was analyzed using a one-way analysis of variance followed by Duncan's multiple range test (SPSS. 19.0 software, IBM Crop.). Results were considered statistically significant at $p < 0.05$. All experiments were performed at least in triplicate, and the results were reported as mean ± standard deviation.

3 | RESULTS AND DISCUSSION

3.1 | Analysis of pH, SSC, water content, and turbidity of fruit pulps and complexes

3.1.1 | Effect of SG on pH, SSC, water content, and turbidity of fruit pulps

pH, SSC, water content, and turbidity of fruit pulps are summarized in Table 1. Fruit pulp showed a low pH (4.02–4.29) and high water content (86.1%–91.79%). Meanwhile, the SSC and turbidity of fruit pulps varied from 6.97 to 11.63 and 174.00 to 244.33, respectively. Among all the fruit pulps, both the lowest pH (4.02) and SSC (6.97) and the highest water content (91.79%) were obtained in the N group. A group with the highest SSC indicated a high sugar and soluble polymer content. However, the highest turbidity (244.33) was obtained in the H group, which might be

TABLE 1 Analysis of pH, soluble solids content (SSC), water content, and turbidity of fruit pulps.

		pH	SSC	Water content	Turbidity
Nectarine pulp group	N	4.02 ± 0.02c	6.97 ± 0.15ie	91.79 ± 0.09%b	198.33 ± 14.57cd
	30N	4.04 ± 0.02c	6.70 ± 0.17f	92.41 ± 0.12%a	182.00 ± 3.00de
	50N	4.09 ± 0.03c	6.50 ± 0.17f	92.20 ± 0.22%ab	214.33 ± 11.51c
Apple pulp group	A	4.14 ± 0.01b	11.63 ± 0.15a	86.10 ± 0.20%f	174.00 ± 4.58e
	30A	4.14 ± 0.01b	11.17 ± 0.15b	86.48 ± 0.07%ef	177.67 ± 3.21e
	50A	4.14 ± 0.01b	11.17 ± 0.06b	86.58 ± 0.28%e	198.67 ± 6.11 cd
Honey peach pulp group	H	4.29 ± 0.02a	7.80 ± 0.10c	90.28 ± 0.28%d	244.33 ± 5.86b
	30H	4.27 ± 0.01a	7.43 ± 0.12d	90.85 ± 0.13%c	266.33 ± 5.13a
	50H	4.27 ± 0.01a	6.60 ± 0.17f	90.71 ± 0.21%cd	236.00 ± 25.36b

Note: Values are averages ± standard deviations. Different lowercase letters indicate significant differences among treatments ($p < 0.05$). N, nectarine pulp; 30N, nectarine pulp with 30 Hz superfine grinding; 50N, nectarine pulp with 50 Hz superfine grinding; A, apple pulp; 30A, apple pulp with 30 Hz superfine grinding; 50A, apple pulp with 50 Hz superfine grinding; H, honey peach pulp; 30H, honey peach pulp with 30 Hz superfine grinding; 50H, honey peach pulp with 50 Hz superfine grinding.

TABLE 2 Analysis of pH, soluble solids content (SSC), water content, and turbidity of complexes.

		pH	SSC	Water content	Turbidity
Nectarine-SPI complex group	N-SPI	5.45 ± 0.02d	11.63 ± 0.35c	81.63 ± 0.18%a	680.00 ± 32.45e
	30N-SPI	5.48 ± 0.03d	10.77 ± 0.50de	82.07 ± 0.26%a	941.67 ± 21.08c
	50N-SPI	5.50 ± 0.05d	10.17 ± 0.60ef	81.86 ± 0.31%a	1021.67 ± 33.72b
Apple-SPI complex group	A-SPI	5.86 ± 0.04b	16.16 ± 0.49a	76.49 ± 0.30%d	657.67 ± 21.39e
	30A-SPI	6.03 ± 0.02a	15.50 ± 0.10a	77.26 ± 0.11%c	986.33 ± 16.01bc
	50A-SPI	5.89 ± 0.02b	14.70 ± 0.61b	77.51 ± 0.14%c	1011.67 ± 39.31b
Honey peach-SPI complex group	H-SPI	5.69 ± 0.02c	10.97 ± 0.15cd	79.64 ± 0.18%b	769.33 ± 14.50d
	30H-SPI	5.69 ± 0.03c	9.83 ± 0.23fg	79.78 ± 0.21%b	1131.00 ± 7.55a
	50H-SPI	5.71 ± 0.02c	9.30 ± 0.36g	80.06 ± 0.06%b	1148.00 ± 31.76a

Note: Values are averages ± standard deviations. Different lowercase letters indicate significant differences among treatments ($p < 0.05$). N-SPI, nectarine pulp-soy protein isolate complex; 30N-SPI, nectarine pulp with 30 Hz superfine grinding-soy protein isolate complex; 50N-SPI, nectarine pulp with 50 Hz superfine grinding-soy protein isolate complex; A-SPI, apple pulp-soy protein isolate complex; 30A-SPI, apple pulp with 30 Hz superfine grinding-soy protein isolate complex; 50A-SPI, apple pulp with 50 Hz superfine grinding; H-SPI, honey peach pulp-soy protein isolate complex; 30H-SPI, honey peach pulp with 30 Hz superfine grinding-soy protein isolate complex; 50H-SPI, honey peach pulp with 50 Hz superfine grinding-soy protein isolate complex.

attributed to the high content of the insoluble components. When subjected to the SG processing, SSC in all the fruit pulp groups was significantly decreased, which could be ascribed to the polysaccharide degradation. The turbidity was remarkably increased in the nectarine pulp group and apple pulp group alongside the SG treatment, which might be attributed to the cell breakage and cell wall polysaccharides dissolution (Huang et al., 2018). Interestingly, except for turbidity, with the increase in SG frequency, pH, SSC, and water content in fruit pulps did not show significant differences.

3.1.2 | Analysis of pH, SSC, water content, and turbidity of complexes

After SPI addition, pH, SSC, and turbidity of the complexes group were considerably increased (Table 2), compared with the fruit pulps group, whereas water content was decreased. Especially, with the increase in SG frequency, SSC in all the complex groups was remarkably declined. This phenomenon could be explained by the exposure of polysaccharides with the increased negative charge induced by SG with high frequency, which could enhance the formation of fruit pulp-SPI insoluble complexes. On another point, the pH of the fruit pulps was near the PI of SPI, which would accelerate the self-aggregation resulting in a high SSC (Jones & McClements, 2011). However, the increased behavior with the increase in SG frequency was found in turbidity. Fruit pulps with a loose and flexible structure induced by SG processing could easily be conjugated with SPI, facilitating the formation of biopolymer particles (de Souza et al., 2009).

In detail, among all the fruit-SPI groups, with the increase in SG frequency, the highest increase rate in turbidity (35%) and water content (1.3%) was observed in the apple-SPI complex group. This might be because the apple polysaccharides unfolded to expose more hydrophobic groups after SG treatment than nectarine and honey peach and therefore aggregated with SPI more easily. The honey peach-SPI complex group showed the highest reduction ratio in SSC (18%). It was speculated that the interaction between SPI and honey peach polysaccharides could enhance the formation of insoluble complexes. Our findings were consistent with the results of Souza and Garcia-Rojas (2015).

3.2 | Analysis of particle size of fruit pulps and complexes

The particle size distributions of fruit pulps and complexes treated by SG are shown in Figure 1. $D[4, 3]$, as the volume-based mean diameter, was mainly affected by the large particles in systems, whereas $D[3, 2]$, as the area-based mean diameter, was mainly affected by the small ones in systems (Augusto et al., 2012).

3.2.1 | Effect of SG on the particle size of fruit pulps

With the increase in SG frequency, $D[3, 2]$ and $D[4, 3]$ were remarkably decreased, resulting from the strong shear stress and high pressure of SG. The most significant declines in $D[3, 2]$ and $D[4, 3]$ were all found in the nectarine pulp group. Furthermore, as a consequence of SG with powerful shear stress, the cell wall polymers might be depolymerized into molecules with a small weight (Huang et al., 2018). Only during the SG with 50 Hz processing, $D[3,$

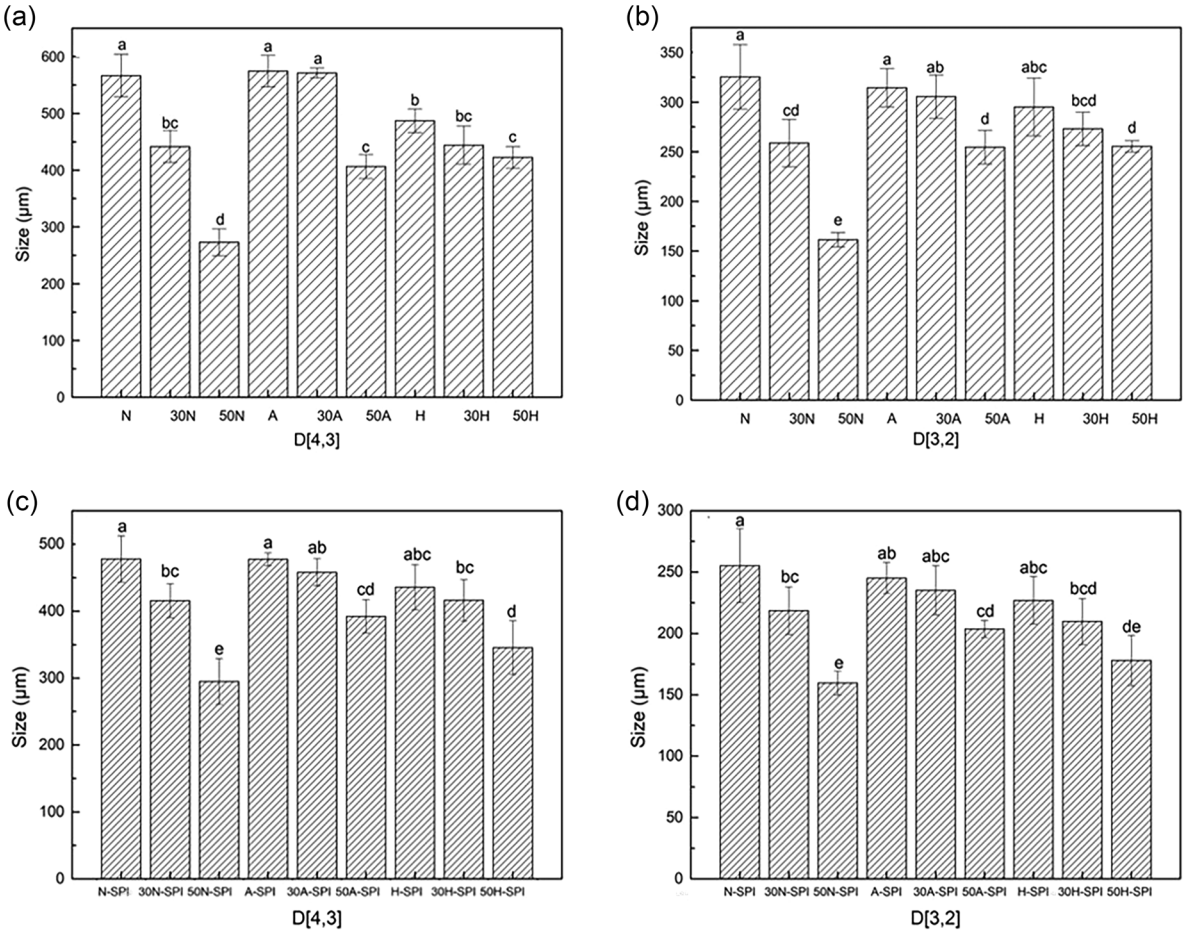

FIGURE 1 Changes in particle size of fruit pulp and complexes: *D*[4,3] of fruit pulps (a); *D*[3,2] of fruit pulps (b); *D*[4,3] of complexes (c); and *D*[3,2] of complexes (d). *Note*: Different lowercase letters indicate significant differences among treatments ($p < 0.05$). N, nectarine pulp; 30N, nectarine pulp with 30 Hz superfine grinding; 50N, nectarine pulp with 50 Hz superfine grinding; A, apple pulp; 30A, apple pulp with 30 Hz superfine grinding; 50A, apple pulp with 50 Hz superfine grinding; H, honey peach pulp; 30H, honey peach pulp with 30 Hz superfine grinding; 50H, honey peach pulp with 50 Hz superfine grinding; N-SPI, N-soy protein isolate complex; 30N-SPI, 30N-soy protein isolate complex; 50N-SPI, 50N-soy protein isolate complex; A-SPI, A-soy protein isolate complex; 30A-SPI, 30A-soy protein isolate complex; 50A-SPI, 50A-soy protein isolate complex; H-SPI, H-soy protein isolate complex; 30H-SPI, 30H-soy protein isolate complex; 50H-SPI, 50H-soy protein isolate complex.

2] and *D*[4, 3] in the apple pulp group showed a significant decrease. Similar behavior of *D*[3, 2] and *D*[4, 3] was also found in the honey peach pulp group. Under the low SG frequency (30 Hz), the inhibitory effect of apple pulp with high SSC content on the decline in particle size should be considered. Meanwhile, when subjected to SG with high frequency (50 Hz), *D*[3, 2] and *D*[4, 3] in apple pulp were significantly decreased, owing to the high shear force.

3.2.2 | Analysis of particle size of complexes

Compared with the fruit pulp group, following SPI addition, the *D*[3, 2] and *D*[4, 3] of complexes were obviously decreased, implying that the pulp particles intensely coated with SPI molecules and formed smaller complexes attributed to the electrostatic interaction. Our observation aligned with the result of Yi et al. (2021), who reported a reduction in the particle size of pea protein following the incorporation of pectin. For the complexes, based on the properties of fruit pulp treated under SG processing with different frequencies, the lowest *D*[3, 2] and *D*[4, 3] were presented in the complexes consisting of the fruit pulp treated with SG at 50 Hz. High-intensity shear stress caused by SG resulted in the degradation of polysaccharides, increasing electronegativity and free carboxylic functional groups (Villay et al., 2012), thereby enhancing electrostatic interactions and tight aggregation between SPI and polysaccharides. The presence of electrostatic interaction of polysaccharides–protein was also described by He et al. (2021). The highest reduction ratio in particle size was also observed in the nectarine-SPI group.

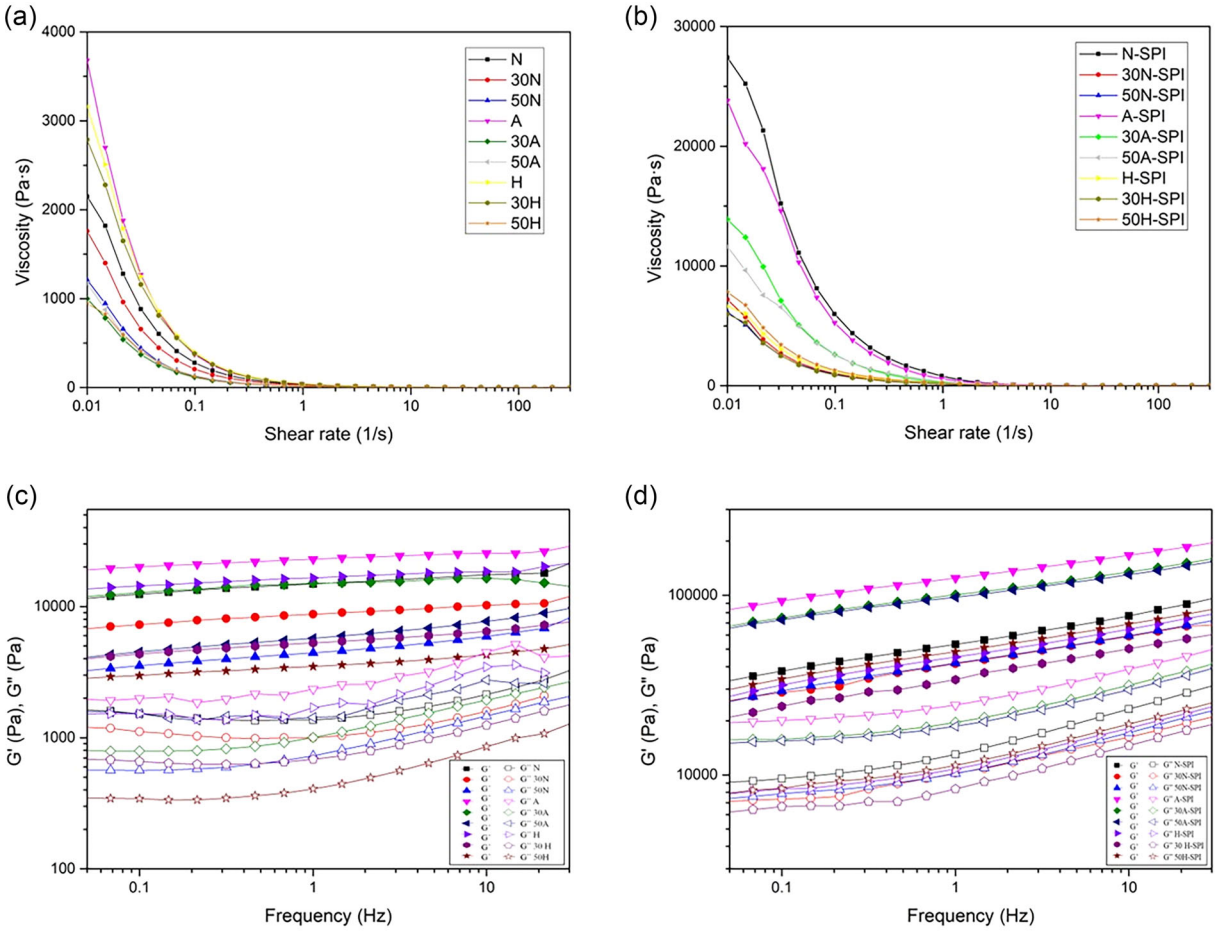

FIGURE 2 The flow curve of shear rate-apparent viscosity of fruit pulps (a); the flow curve of shear rate-apparent viscosity of complexes (b); the evolution of the G' and G'' of fruit pulps (c); and the evolution of the G' and G'' of complexes (d). G', the storage modulus; G'', loss modulus. N, nectarine pulp; 30N, nectarine pulp with 30 Hz superfine grinding; 50N, nectarine pulp with 50 Hz superfine grinding; A, apple pulp; 30A, apple pulp with 30 Hz superfine grinding; 50A, apple pulp with 50 Hz superfine grinding; H, honey peach pulp; 30H, honey peach pulp with 30 Hz superfine grinding; 50H, honey peach pulp with 50 Hz superfine grinding; N-SPI, N-soy protein isolate complex; 30N-SPI, 30N-soy protein isolate complex; 50N-SPI, 50N-soy protein isolate complex; A-SPI, A-soy protein isolate complex; 30A-SPI, 30A-soy protein isolate complex; 50A-SPI, 50A-soy protein isolate complex; H-SPI, H-soy protein isolate complex; 30H-SPI, 30H-soy protein isolate complex; 50H-SPI, 50H-soy protein isolate complex.

Especially, the apple-SPI complexes group showed the lowest reduction ratio in particle size, ascribing to the high homogalacturonan content in apple pectin against the shear rate (Mendez et al., 2023).

3.3 | Analysis of rheological properties of fruit pulps and complexes

3.3.1 | Effect of SG on rheological properties of fruit pulps

All the fruit pulp exhibited the shear thinning behavior, with a significant decrease in viscosity within the shear rate varied from 0.1 to 10 S^{-1}, suggesting excellent flowability. With the increase in SG frequency, the viscosity in all the fruit pulp groups was decreased (Figure 2a), which was explained by the reduction in particle size caused by SG with a high shearing rate. Under the high shear stress circumstance, the depolymerization or disruption in cell wall polymers has been confirmed (Huang et al., 2018), which referred to the decline in viscosity of fruit pulp. Further, the highest viscosity was shown in the A group, followed by the H and the N groups, which might be ascribed to high SSC and high pectin content (Villay et al., 2012).

To identify the viscoelastic behavior of the fruit pulp with SG treatment, a frequency-sweep measurement was applied, and the results are shown in Figure 2c. It could be found that in all the fruit groups, the storage modulus (G') and loss modulus (G'') were quasi-parallel. Meanwhile, the value of G' was much higher than that of G'', indicating that the fruit pulps should be identified as the formation of

gels. Both the G' and G'' increased with frequency, illustrating that the fruit pulp exhibited a predominant solid-like behavior. In addition, the values of G' and G'' declined with the increased SG frequency, suggesting that the texture strength of the fruit pulp was weakened by the SG processing. This corroborated well with the result of the changes in particle size. The changes in the structure properties of polysaccharides resulting from SG treatment with high shear stress and pressure might alter the rheological properties of fruit pulps (Zhao et al., 2009).

3.3.2 | Analysis of rheological properties of complexes

The addition of SPI increased the initial viscosity of the complexes (Figure 2b), which was 10 times higher than that of fruit pulps. It can be explained that SPI, as a binding agent, could cross-link with the components (e.g., polysaccharides) in fruit pulp by the non-covalent bond, which would enhance the gelation capacity and apparent viscosity of the complexes. The observation was also described by Jiang et al. (2020). Moreover, the viscosity of all fruit pulp-SPI complexes reduced with an increased frequency of SG. The strongest reduction was observed in the complexes prepared by fruit pulp treated with SG at 50 Hz, especially for the 50N-SPI group. Nectarine with low SSC was more susceptible to shear force than apple pulp.

The values of G' and G'' of fruit pulp-SPI complexes were increased compared to fruit pulps (Figure 2d), illustrating the enhanced shape retention stability and the mechanical strength of the complexes under the SPT-treated strategy. It was suggested that the cell wall polysaccharides might be partially depolymerized when SG was treated, accompanied by the exposure of optimal amounts of –OH groups. Thus, the friction and entanglement between the cell wall polysaccharides and the SPI through covalent disulfide bond and ionic bond were enhanced, as well as the values of G' and G'' (Phuhongsung et al., 2020). In all the fruit pulp-SPI complexes, G' was much higher than G'' within the range of 0.1–10 Hz, indicating the fruit pulp-SPI complexes exhibited a typical gel-like behavior (Huang et al., 2020).

With the increase in frequency, G' and G'' were gradually increased. Specially, within the low frequency (0.1–1 Hz), G'' values increased slowly. However, G'' values showed a sharp increase within the high frequency (1–10 Hz), suggesting that gels had an excellent response to the frequency. When SPI was applied to fruit pulp treated with different SG frequencies, both the values of G' and G'' were decreased, which was attributed to SPI integrating with more flexible components in pulps. As expected, the apple-SPI complexes group exhibited the largest values of G' and G'', followed by honey peach-SPI complex group and nectarine-SPI complexes group, indicating more junction regions in apple-SPI complexes.

3.4 | Analysis of the microstructure of fruit pulps and complexes

3.4.1 | Effect of SG on the microstructure of fruit pulps

The effect of SG processing with different frequencies on the microstructure of fruit pulps was studied and shown in Figure 3a. The honeycomb-like microstructure with uniform big pores was observed in the N group. With the increase in SG frequency, the loose cross-linking network and less ordered structures were obtained in the nectarine pulp, illustrating the damaged cell structure during SG process. A group had a uniform and dense microstructure with small pores, which could capture water molecules easily (Wang et al., 2020). The nonuniform and rough layer structure with the discontinuous agglomerate accumulations were monitored in apple pulp with SG treatment. The obviously sheetlike structure with large pores was found in the H group. However, the sheetlike structure conversed into some aggregates when subjected to SG treatment with 30 Hz. Under high SG frequency (50 Hz), the disordered sheetlike structure was formed, which might be attributed to high shear force and high pressure.

3.4.2 | Analysis of the microstructure of complexes

With the exposure of the globular protein structure of SPI (Figure S1) resulted from heating processing, the N-SPI, A-SPI, and H-SPI complexes showed the three-dimensional gel microstructure, in which the denatured SPI particles were observed. SPI embedded into the network of fruit pulp might interact with the cell wall polysaccharides or other substances with small molecules, which would affect the changes in microstructures of fruit pulps. For the fruit pulp-SPI complexes, the SPI aggregated and filaments coexisted together. Furthermore, the presence of polysaccharides in fruit pulps might lead to the formation of porous gel structures based on the electrostatic interaction, which was also described by He et al. (2021).

The modification of structure in fruit pulps induced by the SG treatment at 30 Hz might increase the actual number of active sites (e.g., hydrophobic sites) in cell wall polysaccharides, which could be recognized by SPI. Therefore, stable, uniform, and dense microstructures were observed. However, when SPI was applied to the fruit pulps

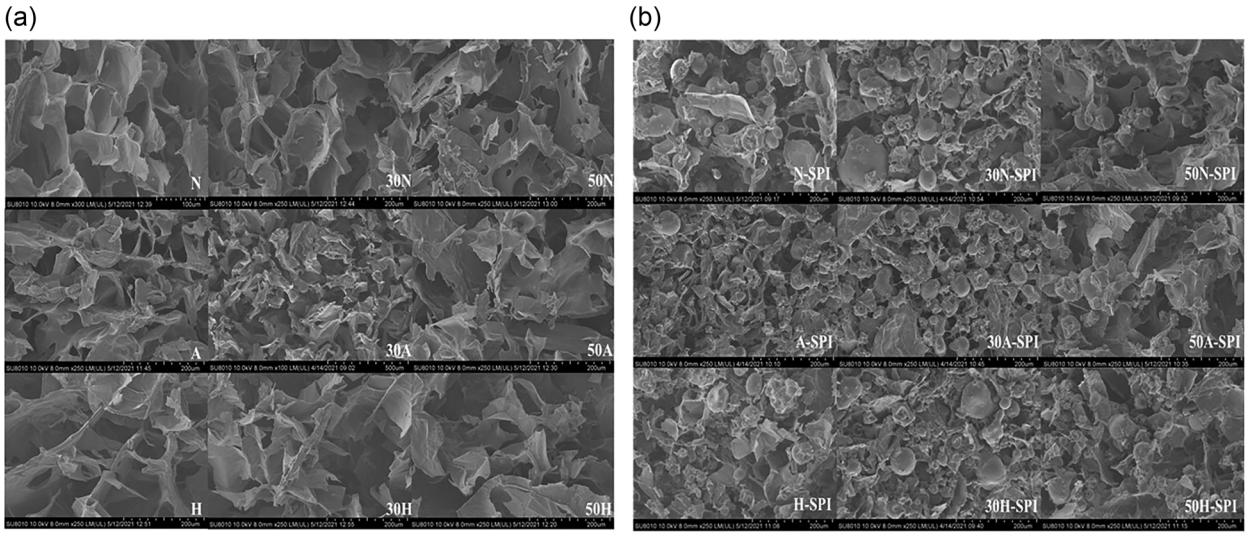

FIGURE 3 The scanning electron microscope (SEM) images: fruit pulps (a) and complexes (b). SEM, scanning electron microscope; N, nectarine pulp; 30N, nectarine pulp with 30 Hz superfine grinding; 50N, nectarine pulp with 50 Hz superfine grinding; A, apple pulp; 30A, apple pulp with 30 Hz superfine grinding; 50A, apple pulp with 50 Hz superfine grinding; H, honey peach pulp; 30H, honey peach pulp with 30 Hz superfine grinding; 50H, honey peach pulp with 50 Hz superfine grinding; N-SPI, N-soy protein isolate complex; 30N-SPI, 30N-soy protein isolate complex; 50N-SPI, 50N-soy protein isolate complex; A-SPI, A-soy protein isolate complex; 30A-SPI, 30A-soy protein isolate complex; 50A-SPI, 50A-soy protein isolate complex; H-SPI, H-soy protein isolate complex; 30H-SPI, 30H-soy protein isolate complex; 50H-SPI, 50H-soy protein isolate complex.

with SG treatment at 50 Hz, a disordered and discontinuous structure with large pores was obtained, consistent with the microstructure of fruit pulps treated with SG processing at 50 Hz. Noticeably, the spheroidal SPI particle almost disappeared in complexes in which fruit pulps were treated by SG with 50 Hz. It was reasonable to conclude that SG with high sheer stress could enable the SPI-cell wall polysaccharides interactions and inflect on the weakened textural properties of the complexes gel (Zhao et al., 2009). In particular, the apple-SPI complexes group showed a dense structure corresponding with the high G' and G''. In this regard, modified apple pulp preferentially exposed their hydrophobic group from polysaccharides to SPI, promoting the interaction between polysaccharides and SPI.

3.5 | Analysis of FT-IR spectrum of fruit pulps and complexes

Figure 4 illustrates the FT-IR spectrum of all samples. The broad and intense absorption peak around 3375–3383 cm^{-1} has been reported to signify the O–H stretching vibration and N–H stretching vibration with hydrogen-bonded. The absorption peak around 2920–2940 cm^{-1} was identified to characterize the C–H stretching vibration. In addition, the peaks observed around 1650–1750, 1600–1500, and 1250 cm^{-1} were related to the amides I–III, respectively, which resulted from C = O stretching, C–N stretching/in-plane N–H bending, and the C–N stretching/N–H bending, respectively (Ran & Yang, 2022). Peaks around 1540–1180 and 1180–953 cm^{-1} were characterized by the spectrum for the carbohydrate and pectin, respectively (Gu et al., 2010).

3.5.1 | Analysis of FT-IR spectrum of fruit pulps

With the increase in SG frequency, the peak of hydrogen bonding (3375–3383 cm^{-1}) showed a significant right shift, indicating the enhanced hydrogen bonding intensity. The right-shifted changes in 1629 cm^{-1} indicating the considerable exposure of carboxylic groups (COO^-) from the polysaccharide could accelerate the electrostatic interactions, which was beneficial for gel forming. Compared with apple pulp and honey peach pulp without SG processing, the nectarine pulp had a broader peak at 3375 cm^{-1} and right shifted significantly, suggesting a stronger hydrogen bonding. The peak around 1740 cm^{-1} was clearly displayed in the nectarine and honey peach pulp, which has been reported to signify the C = O stretching (Wang et al., 2023). However, no obvious peak around 1740 cm^{-1} in the apple pulp was observed. Meanwhile, a broad peak around 1630 cm^{-1} in apple pulp was ascribing ascribed to COO^-. The strong band around 846 cm^{-1} was observed in the apple group, which was considered the

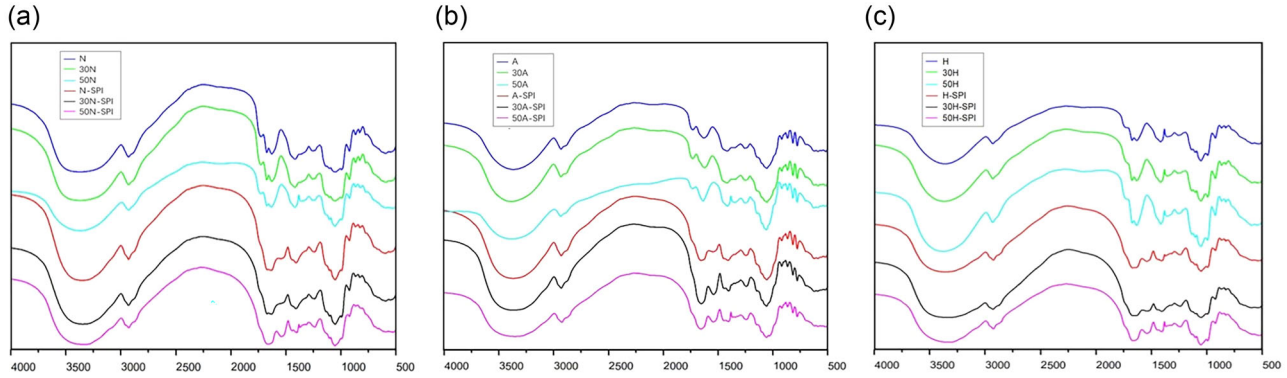

FIGURE 4 Fourier transform infrared (FT-IR) spectra; nectarine pulps and nectarine-SPI complexes (a); apple pulps and apple-SPI complexes (b); and honey peach pulps and honey peach-SPI complexes (c). N, nectarine pulp; 30N, nectarine pulp with 30 Hz superfine grinding; 50N, nectarine pulp with 50 Hz superfine grinding; A, apple pulp; 30A, apple pulp with 30 Hz superfine grinding; 50A, apple pulp with 50 Hz superfine grinding; H, honey peach pulp; 30H, honey peach pulp with 30 Hz superfine grinding; 50H, honey peach pulp with 50 Hz superfine grinding; N-SPI, N-soy protein isolate complex; 30N-SPI, 30N-soy protein isolate complex; 50N-SPI, 50N-soy protein isolate complex; A-SPI, A-soy protein isolate complex; 30A-SPI, 30A-soy protein isolate complex; 50A-SPI, 50A-soy protein isolate complex; H-SPI, H-soy protein isolate complex; 30H-SPI, 30H-soy protein isolate complex; 50H-SPI, 50H-soy protein isolate complex.

characteristic band for the D-galactose-4-sulfate (Mao et al., 2023). Moreover, the nectarine and honey peach groups showed a strong intensity peak around 927 cm^{-1}, which was the characteristic band for 3,6-anhydro-D-galactose.

3.5.2 | Analysis of FT-IR spectrum of complexes

Compared to nectarine pulps, the peaks in nectarine-SPI complexes around 1730 and 1640 cm^{-1} disappeared. The peak around 1535 cm^{-1} was observed in the nectarine-SPI complexes, related to the N–H bending of amide II (Zhang et al., 2021). As for the apple-SPI complexes, the absorption peaks around 2920 cm^{-1} were attributed to C–H stretching bands of the polysaccharides. Moreover, the N–H bending corresponding to amide II of apple-SPI complexes was shifted to 1540 cm^{-1}. An absorption peak at 1645 cm^{-1} indicated the free carboxyl groups in honey peach-SPI complexes, whereas the absorption peaks at 1530 cm^{-1} corresponded to N–H bending of amide II, which could be ascribed to the formation of new complexes compared with honey peach pulps (Jiang et al., 2020). For all fruit pulp-SPI complexes, when subjected to SPI addition, there was a considerable right shift of the broad absorption bands of the O–H stretching and C–H stretching vibrations, indicating the enhanced interactions between SPI and polysaccharides from fruit pulps through intermolecular hydrogen bond (Ran et al., 2022). Compared with the fruit pulps, the carboxyl absorptions with broader peaks (1700–1560 cm^{-1}) were observed in fruit pulp-SPI complexes, highlighting the stronger electrostatic interaction between SPI and COO^- a group of fruit pulps. The new peak at 1540 cm^{-1} was observed in all complexes, which illustrated the C–N stretching vibration, as well as the formation of the new substance (Boostani et al., 2017).

3.6 | Analysis of texture properties of complexes

Gel strength was defined as the maximum force during the sustained compression (Zhuang et al., 2019). The highest gel strength was observed in the A-SPI group (648.18 g), followed by H-SPI and N-SPI groups (Figure 5a). When subjected to SG processing, the gel strengths in the nectarine-SPI complexes group and apple-SPI complexes group were significantly decreased, attributing to the flexible and loose structure (Huang et al., 2020). However, no significant differences were observed in the honey peach-SPI complexes group, in which honey peach pulps were prepared under different SG treatments, corroborating well with the results on the viscosity. Moreover, the smallest reduction was found in honey peach pulp under the distinct SG processing compared to the apple-SPI complexes group and nectarine-SPI complexes group. Adhesiveness referred to the required energy to maintain the network structure (Huang et al., 2020). The highest adhesiveness was performed in the apple-SPI complexes group varied from 7974 to 6204 g s (Figure 5b). The impact of SG modification on apple pulps induced the increase in adhesiveness of apple-SPI complexes, although no significant differences were performed in the 30A-SPI group and 50A-SPI group. It could be explained that the SG improved the exposure of hydrophobic groups in

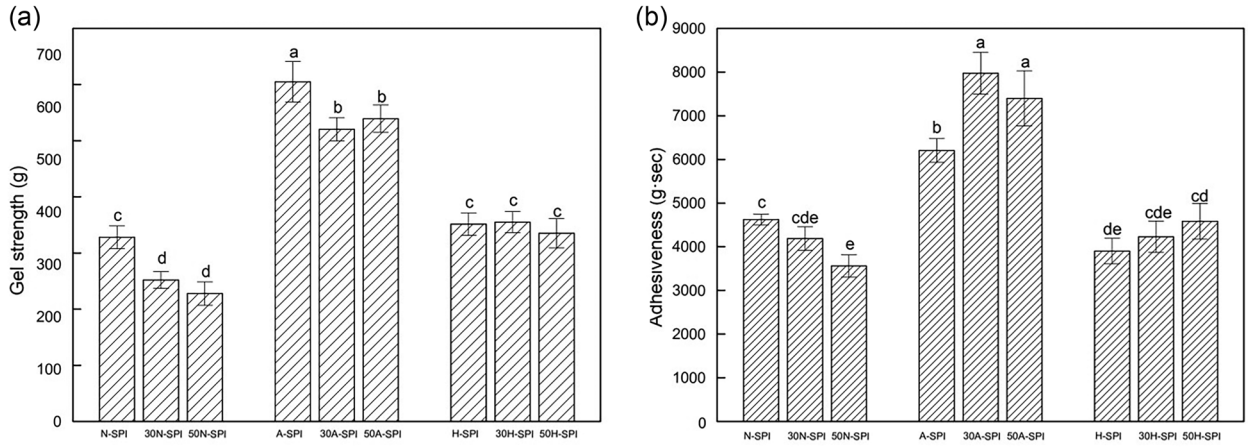

FIGURE 5 Analysis of texture properties of complexes: the gel strength of complexes (a) and the adhesiveness of complexes (b). *Note*: Different lowercase letters indicate significant differences among treatments ($p < 0.05$). N-SPI, nectarine pulp-soy protein isolate complex; 30N-SPI, nectarine pulp with 30 Hz superfine grinding-soy protein isolate complex; 50N-SPI, nectarine pulp with 50 Hz superfine grinding-soy protein isolate complex; A-SPI, apple pulp-soy protein isolate complex; 30A-SPI, apple pulp with 30 Hz superfine grinding-soy protein isolate complex; 50A-SPI, apple pulp with 50 Hz superfine grinding; H-SPI, honey peach pulp-soy protein isolate complex; 30H-SPI, honey peach pulp with 30 Hz superfine grinding-soy protein isolate complex; 50H-SPI, honey peach pulp with 50 Hz superfine grinding-soy protein isolate complex.

polysaccharides and reinforced the intermolecular force between SPI and substances in apple pulp, resulting in a compact network structure (Jiang et al., 2020). Conversely, with the increased SG frequency, the adhesiveness of the nectarine-SPI complexes group was decreased, corresponding to the low viscosity of 50N. Meanwhile, no apparent alterations were observed in the adhesiveness of the honey peach-SPI complex group with SG processing.

3.7 | Analysis of WHC of complexes

WHC highly depended on the gel microstructure, which could wrap the moisture. As shown in Figure 6, the highest WHC was illustrated in the apple-SPI group, followed by the honey peach-SPI and nectarine-SPI groups. There might be two reasonable explanations: First, the high apparent viscosity and uniform structure with small pore size in apple-SPI complexes could attract moisture tightly (Ma et al., 2020). Additionally, the polysaccharides (e.g., pectin) in apple pulp with high content and high molecular weight were preferred to enhance the formation of dense networks as well as the rheological properties. When SPI was applied to apple fruit pulp treated by SG with 50 Hz, WHC was significantly decreased, whereas SG did not show a remarkable effect on nectarine-SPI and honey peach-SPI complexes. It was reasonable to conclude that the different effects of SG processing on WHC might be owed to the higher branching degree of peach pectin and degree of esterification, which had a greater resistance to shear stress than apple (Xia et al., 2019).

3.8 | Analysis of water distribution of complexes

The water distribution and water mobility of the fruit pulp-SPI complexes were analyzed by IF-NMR. Relaxation time (T_2) was used to describe the binding force and the degree of freedom of hydrogen protons in samples. As shown in Figure 7, three distinct regions were separated based on the T_2 within 0.01–10,000 ms. The region I corresponded to the hydration monolayer, which was bound to the sample by strong hydrogen bonding. Therefore, T_{21} was related to the water captured in the cell wall, which occurred due to the chemical exchange effects related to rapid proton exchange between water and hydroxyl protons on rigid cell wall polysaccharides (pectin, cellulose, and hemicellulose). Region II, including T_{22} and T_{23}, was attributed to immobilized water that existed in the cytoplasm, which was strongly bonded to the monolayer water molecules. T_{22} and T_{23} were related to the chemical exchange between water and proteins of the cytoskeleton and enzymes, as well as the high viscosity of cell membranes. T_{24}, labeled in region III, represented free water, weakly bound to food (Luo et al., 2020). T_{23} was the main water in complexes, whereas only a few T_{21} and T_{24} were represented in the complexes, especially the T_{24}. This might be ascribed to the swelling of SPI, which could wrap the free water and inhibit the mobility of moisture (Peters et al., 2017). Additionally, the conversion between free water (T_{24}) and immobilized water (T_{23}) in complexes was observed with the increased SG frequency, suggesting a decrease in the number and freedom of hydrogen protons (Han et al.,

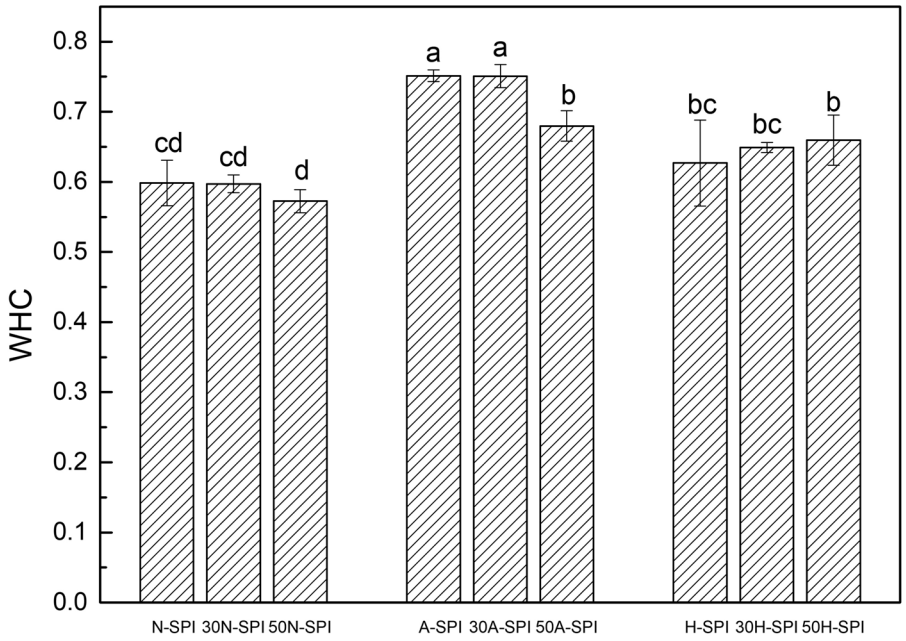

FIGURE 6 Analysis of water-holding capacity (WHC) of complexes. *Note*: Different lowercase letters indicate significant differences among treatments ($p < 0.05$). N-SPI, nectarine pulp-soy protein isolate complex; 30N-SPI, nectarine pulp with 30 Hz superfine grinding-soy protein isolate complex; 50N-SPI, nectarine pulp with 50 Hz superfine grinding-soy protein isolate complex; A-SPI, apple pulp-soy protein isolate complex; 30A-SPI, apple pulp with 30 Hz superfine grinding-soy protein isolate complex; 50A-SPI, apple pulp with 50 Hz superfine grinding; H-SPI, honey peach pulp-soy protein isolate complex; 30H-SPI, honey peach pulp with 30 Hz superfine grinding-soy protein isolate complex; 50H-SPI, honey peach pulp with 50 Hz superfine grinding-soy protein isolate complex.

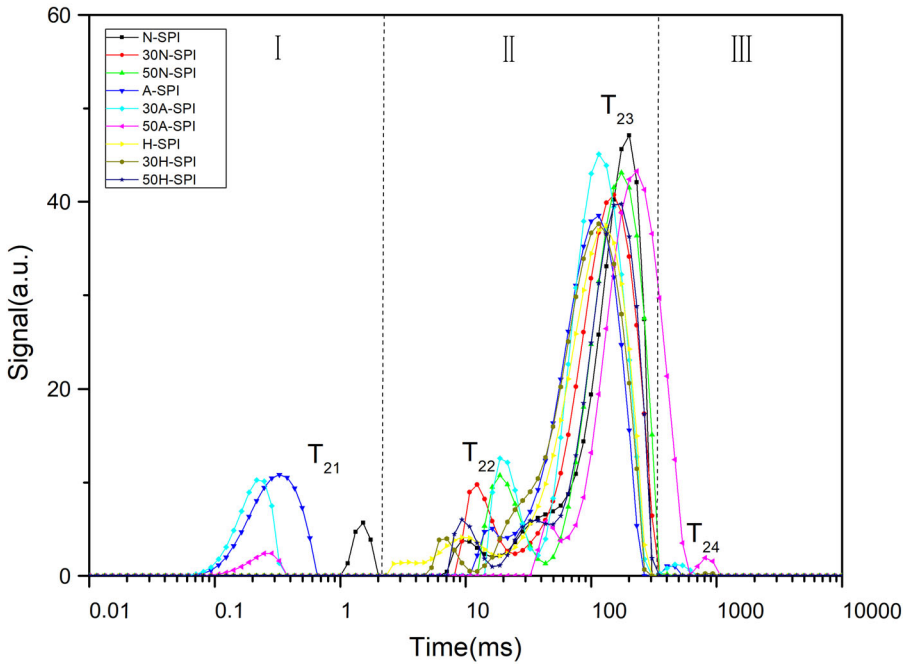

FIGURE 7 Analysis of distributed water relaxation times (T_2) of complexes. N-SPI, nectarine pulp-soy protein isolate complex; 30N-SPI, nectarine pulp with 30 Hz superfine grinding-soy protein isolate complex; 50N-SPI, nectarine pulp with 50 Hz superfine grinding-soy protein isolate complex; A-SPI, apple pulp-soy protein isolate complex; 30A-SPI, apple pulp with 30 Hz superfine grinding-soy protein isolate complex; 50A-SPI, apple pulp with 50 Hz superfine grinding; H-SPI, honey peach pulp-soy protein isolate complex; 30H-SPI, honey peach pulp with 30 Hz superfine grinding-soy protein isolate complex; 50H-SPI, honey peach pulp with 50 Hz superfine grinding-soy protein isolate complex.

TABLE 3 Sensory evaluation of complexes.

	Color	Flavor	Texture	Overall evaluation
N-SPI	6.73 ± 0.82a	5.33 ± 0.49ab	7.13 ± 0.67ab	7.80 ± 0.62abc
30N-SPI	6.57 ± 0.68a	5.27 ± 0.70abc	7.13 ± 0.67ab	7.87 ± 0.79ab
50N-SPI	6.53 ± 0.69a	4.97 ± 0.69bcd	6.03 ± 0.52e	7.70 ± 0.56bc
A-SPI	5.97 ± 0.77bc	5.60 ± 0.66a	7.57 ± 0.96a	8.33 ± 0.67a
30A-SPI	6.40 ± 0.69ab	5.37 ± 0.92ab	7.60 ± 0.69a	7.90 ± 0.66ab
50A-SPI	6.40 ± 0.67ab	4.83 ± 0.59bcd	6.87 ± 1.02bc	7.33 ± 0.82bcd
H-SPI	5.77 ± 0.62c	4.77 ± 0.65cd	6.57 ± 0.68bcd	7.47 ± 0.58bc
30H-SPI	5.93 ± 0.65bc	4.83 ± 0.62bcd	6.47 ± 0.81de	7.27 ± 0.84cd
50H-SPI	5.77 ± 0.72c	4.59 ± 0.54d	6.13 ± 0.71e	6.86 ± 0.71d

Note: Values are averages ± standard deviations. Different lowercase letters indicate significant differences among treatments ($p < 0.05$). N-SPI, nectarine pulp-soy protein isolate complex; 30N-SPI, nectarine pulp with 30 Hz superfine grinding-soy protein isolate complex; 50N-SPI, nectarine pulp with 50 Hz superfine grinding-soy protein isolate complex; A-SPI, apple pulp-soy protein isolate complex; 30A-SPI, apple pulp with 30 Hz superfine grinding-soy protein isolate complex; 50A-SPI, apple pulp with 50 Hz superfine grinding; H-SPI, honey peach pulp-soy protein isolate complex; 30H-SPI, honey peach pulp with 30 Hz superfine grinding-soy protein isolate complex; 50H-SPI, honey peach pulp with 50 Hz superfine grinding-soy protein isolate complex.

2008). Compared with the N-SPI group, T_{23} in 30N-SPI group was left-shifted, suggesting decreased fluidity of immobilized water. This moisture would bind more tightly to cell wall material. As SG frequency increased, the bonding capacity toward moisture was enhanced because of the exposure of –OH after SG processing. As for apple-SPI complexes group, no significant change of T_{23} in 30A-SPI group was observed with SG treatment. However, T_{22} and T_2 of 50A-SPI group showed a significant right shift, contributing to the degradation of polysaccharides and the destruction of cells with SG. Meanwhile, the area value of T_{21} in 50A-SPI group showed a remarkable decrease, attributing to the reduction of bound water. In the case of honey peach-SPI complexes group, T_{23} of 50H-SPI group experienced a right shift, illustrating the increase in the fluidity of this immobilized water, which could be explained by the excessively damaged cell wall material in honey peach by SG processing with 50 Hz. However, T_{22} in 30H-SPI group was left shifted, attributing to the exposure of –OH during SG processing. The shortest T_2 was demonstrated in apple-SPI complexes group, indicating the strongest water binding capacity, which was also reflected in the results of WHC.

3.9 | Sensory evaluation

Sensory outcomes are grouped in Table 3. The color scores were ranged from 6.73 (N-SPI) to 5.77 (H-SPI and 50H-SPI). No significant differences were found in color within the same fruit sample group, which suggested that SG with different frequencies did not remarkably affect the color. Notably, the color scores of nectarine-SPI samples were significantly higher than that of honey peach-SPI samples, illustrating that honey peach pulp was more prone to oxidation and discoloration. As for the flavor evaluation, the statistical significance was only obtained among 50A-SPI, A-SPI, and 30A-SPI. However, the flavor scores did not show the statistical significance among the peach groups. For texture evaluation, samples with SG at high frequency (50 Hz) obtained the lowest scores, indicating the destructed texture. Finally, in terms of the overall evaluation, the highest score was achieved in A-SPI sample, followed by 30A-SPI, 30N-SPI, and N-SPI samples. The result was also supported by the results of gel strength and WHC results. Taken together, the semisolids with gel networks for the elderly prepared by fruit pulp and SPI could be acceptable, which could be modified by SG technology.

3.10 | Correlation analysis

To illustrate the connection between the complexes and fruit pulps, a correlation analysis was performed (Figure 8). G' of complexes was positively correlated with SSC, D[4, 3], and G' of pulps, whereas it was negatively correlated with turbidity and water content of the pulp. WHC of complexes was positively correlated with SSC, D[4, 3], D[3, 2], and G' of pulp, whereas it was negatively correlated with the water content of the pulp. The hardness of the complexes showed a positive correlation with SSC, D[4, 3], D[3, 2], and G' of pulp, but a negative correlation with the water content of pulp. The adhesiveness of complexes was positively correlated with the SSC of pulps, whereas negatively correlated with water content and turbidity of pulps. The viscosity of complexes was positively correlated with D[4, 3], D[3, 2], and G' of pulp. However, the turbidity of complexes was negatively correlated with D[4, 3], D[3, 2], viscosity, and G' of pulp. There was no significant

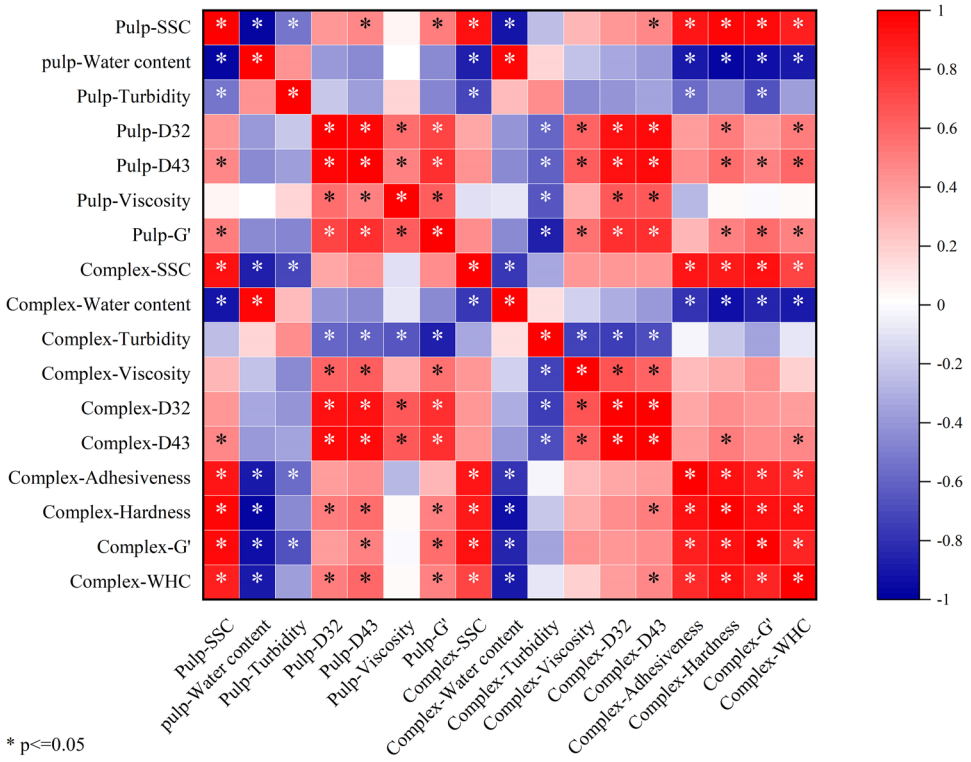

FIGURE 8 Correlation coefficients (heatmap) of various indicators of fruit pulps and the complexes. G'', loss modulus; G', the storage modulus; SSC, soluble solids content; WHC, water-holding capacity.

correlation between the textural properties of the complex and the viscosity of the pulp. This result reflected a strong correlation between fruit pulp and the complexes, representing flexible aggregates with unique properties. Under SG circumstances, the macromolecules in fruit pulp unfolded to provide considerable active sites for SPI, corresponding to the dense structure in the complex system.

4 | CONCLUSION

In this study, SG as the grinding technology was applied for fruit pulps modification. The results confirmed that the characteristics of fruit pulp complexes were significantly affected by the changes in particle size, viscosity, SSC, and rheology properties of fruit pulps. The SG-treated strategy was applied to modify the properties and structure of fruit pulps. As expected, fruit pulps with different molecular bases showed evident differences in the textural and physiochemical properties, which significantly affected the interaction between fruit pulps and SPI. SG with high shear pressure reduced the decline in the particle size accompanied by the exposure of the active site, which would be preferred for interaction with SPI. Especially, moderate changes were shown in fruit pulps under SG with 30 Hz, which was corresponding to the small particle size, high flowability, and great gelation capacity. However, SG with 50 Hz induced excessive destruction in cell structure, resulting in a reduction of viscosity, WHC, textual properties, and stability of the fruit pulps. In this regard, SG with the moderated shear frequency was capable of improving the textural and rheological properties of the fruit pulps as a result of their unique structures. Following SPI addition, the viscoelastic properties of the complexes were pronounced increased, which reflected on gel properties at macro level. In addition, when subjected to SPI, the uniform and dense texture, the enhanced gelation capacities were monitored in fruit pulp-SPI complexes, in which fruit pulp was prepared by SG with 30 Hz. Furthermore, macromolecular substances in fruit pulp with opened structure resulted by SG processing were benefit for the dense structure formation of the fruit pulp-SPI complexes. Sensory evaluation analysis also confirmed the acceptable color, flavor, and texture qualities of the complex gels. Taken together, these findings may expand the application of SG and provide new information on the semisolids with gel networks, which are beneficial for the elderly.

AUTHOR CONTRIBUTIONS

Jin Xie: Conceptualization; methodology; software; data curation; writing—original draft. **Jian Lyu**: Writing—review and editing; funding acquisition;

supervision. **Fengzhao Wang**: Writing—review and editing. **Lansha Bai**: Formal analysis. **Jinfeng Bi**: Funding acquisition; project administration; supervision.

ACKNOWLEDGMENTS

The research was supported by China Agriculture Research System (CARS-30-5-02) and the Agricultural Science and Technology Innovation Program of Institute of Food Science and Technology, Chinese Academy of Agricultural Sciences (CAAS-ASTIP-Q2022-IFST-15).

CONFLICT OF INTEREST STATEMENT

We declare that we do not have any commercial or associative interest that represents a conflict of interest in connection with the work submitted.

ORCID

Jinfeng Bi https://orcid.org/0000-0001-8664-8788

REFERENCES

AOAC. (2005). *Official methods of analysis* (16th ed.). Association of Official Analytical Chemists.

Augusto, P. E. D., Ibarz, A., & Cristianini, M. (2012). Effect of high pressure homogenization (HPH) on the rheological properties of tomato juice: Time-dependent and steady-state shear. *Journal of Food Engineering*, *111*(4), 570–579. https://doi.org/10.1016/j.foodres.2013.06.027

Boostani, S., Aminlari, M., Moosavi-Nasab, M., Niakosari, M., & Mesbahi, G. (2017). Fabrication and characterisation of soy protein isolate-grafted dextran biopolymer: A novel ingredient in spray-dried soy beverage formulation. *International Journal of Biological Macromolecules*, *102*, 297–307. https://doi.org10.1016/j.ijbiomac.2017.04.019

Çakır, E., & Foegeding, E. A. (2011). Combining protein microphase separation and protein–polysaccharide segregative phase separation to produce gel structures. *Food Hydrocolloids*, *25*(6), 1538–1546. https://doi.org/10.1016/j.foodhyd.2011.02.002

Chen, Y., Zhang, M., & Phuhongsung, P. (2021). 3D printing of protein-based composite fruit and vegetable gel system. *LWT—Food Science and Technology*, *141*, 110978. https://doi.org/10.1016/j.lwt.2021.110978<./bib>

de Souza, H. K. S., Bai, G., Gonçalves, M. P., & Bastos, M. (2009). Whey protein isolate–chitosan interactions: A calorimetric and spectroscopy study. *Thermochimica Acta*, *495*(1–2), 108–114. https://doi.org/10.1016/j.tca.2009.06.008

Godoi, F. C., Bhandari, B. R., & Prakash, S. (2017). Tribo-rheology and sensory analysis of a dairy semi-solid. *Food Hydrocolloids*, *70*, 240–250. https://doi.org/10.1016/j.foodhyd.2017.04.011

Gu, F.-L., Kim, J. M., Abbas, S., Zhang, X.-M., Xia, S.-Q., & Chen, Z.-X. (2010). Structure and antioxidant activity of high molecular weight Maillard reaction products from casein–glucose. *Food Chemistry*, *120*(2), 505–511. https://doi.org/10.1016/j.foodchem.2009.10.044

Han, M., Zhang, Y., Fei, Y., Xu, X., & Zhou, G. (2008). Effect of microbial transglutaminase on NMR relaxometry and microstructure of pork myofibrillar protein gel. *European Food Research and Technology*, *228*(4), 665–670. https://doi.org/10.1007/s00217-008-0976-x

He, Z. D., Liu, C. Q., Zhao, J., Li, W. W., & Wang, Y. S. (2021). Physicochemical properties of a ginkgo seed protein-pectin composite gel. *Food Hydrocolloids*, *118*, 106781. https://doi.org/10.1016/j.foodhyd.2021.106781

Huang, M. S., Zhang, M., Bhandari, B., & Liu, Y. (2020). Improving the three-dimensional printability of taro paste by the addition of additives. *Journal of Food Process Engineering*, *43*(5), e13090. https://doi.org/10.1111/jfpe.13090

Huang, X., Dou, J. Y., Li, D., & Wang, L. J. (2018). Effects of superfine grinding on properties of sugar beet pulp powders. *LWT—Food Science and Technology*, *87*, 203–209. https://doi.org/10.1016/j.lwt.2017.08.067

International Organization for Standardization (ISO). (2016). *Sensory analysis—methodology—general guidance for establishing a sensory profile* (ISO Standard No. ISO PN-EN ISO 13299:2016).

Jiang, L., Ren, Y., Xiao, Y., Liu, S., Zhang, J., Yu, Q., Chen, Y., & Xie, J. (2020). Effects of *Mesona chinensis* polysaccharide on the thermostability, gelling properties, and molecular forces of whey protein isolate gels. *Carbohydrate Polymers*, *242*, 116424. https://doi.org/10.1016/j.carbpol.2020.116424

Jones, O. G., & McClements, D. J. (2011). Recent progress in biopolymer nanoparticle and microparticle formation by heat-treating electrostatic protein–polysaccharide complexes. *Advances in Colloid and Interface Science*, *167*(1–2), 49–62. https://doi.org/10.1016/j.cis.2010.10.006

Laguna, L., Hetherington, M. M., Chen, J., Artigas, G., & Sarkar, A. (2016). Measuring eating capability, liking and difficulty perception of older adults: A textural consideration. *Food Quality and Preference*, *53*, 47–56. https://doi.org/10.1016/j.foodqual.2016.05.013

Li, J., Huang, Y., Peng, X., Luo, W., Gantumur, M.-A., Jiang, Z., & Hou, J. (2023). Physical treatment synergized with natural surfactant for improving gas–water interfacial behavior and foam characteristics of α-lactalbumin. *Ultrasonics Sonochemistry*, *95*, 106369. https://doi.org/10.1016/j.ultsonch.2023.106369

Liu, J., Shim, Y. Y., Shen, J., Wang, Y., & Reaney, M. J. T. (2017). Whey protein isolate and flaxseed (*Linum usitatissimum* L.) gum electrostatic coacervates: Turbidity and rheology. *Food Hydrocolloids*, *64*, 18–27. https://doi.org/10.1016/j.foodhyd.2016.10.006

Luo, H., Guo, C., Lin, L., Si, Y., Gao, X., Xu, D., Jia, R., & Yang, W. (2020). Combined use of rheology, LF-NMR, and MRI for characterizing the gel properties of hairtail surimi with potato starch. *Food and Bioprocess Technology*, *13*(4), 637–647. https://doi.org/10.1007/s11947-020-02423-y

Ma, X., Chen, W., Yan, T., Wang, D., Hou, F., Miao, S., & Liu, D. (2020). Comparison of citrus pectin and apple pectin in conjugation with soy protein isolate (SPI) under controlled dry-heating conditions. *Food Chemistry*, *309*, 125501. https://doi.org/10.1016/j.foodchem.2019.125501

Mao, Y., Huang, M., Bi, J., Sun, D., Li, H., & Yang, H. (2023). Effects of kappa-carrageenan on egg white ovalbumin for enhancing the gelation and rheological properties via electrostatic interactions. *Food Hydrocolloids*, *134*, 108031. https://doi.org/10.1016/j.foodhyd.2022.108031

Mendez, D. A., Schroeter, B., Martinez-Abad, A., Fabra, M. J., Gurikov, P., & Lopez-Rubio, A. (2023). Pectin-based aerogel particles for drug delivery: Effect of pectin composition on aerogel structure and release properties. *Carbohydrate Polymers*, *306*, 120604. https://doi.org/10.1016/j.carbpol.2023.120604

Moelants, K. R. N., Jolie, R. P., Palmers, S. K. J., Cardinaels, R., Christiaens, S., Van Buggenhout, S., Van Loey, A. M., Moldenaers, P., & Hendrickx, M. E. (2012). The effects of process-induced pectin changes on the viscosity of carrot and tomato sera. *Food and Bioprocess Technology*, *6*(10), 2870–2883. https://doi.org/10.1007/s11947-012-1004-5

Munialo, C. D., van der Linden, E., Ako, K., Nieuwland, M., Van As, H., & de Jongh, H. H. J. (2016). The effect of polysaccharides on the ability of whey protein gels to either store or dissipate energy upon mechanical deformation. *Food Hydrocolloids*, *52*, 707–720. https://doi.org/10.1016/j.foodhyd.2015.08.013

Peters, J. P. C. M., Vergeldt, F. J., Boom, R. M., & van der Goot, A. J. (2017). Water-binding capacity of protein-rich particles and their pellets. *Food Hydrocolloids*, *65*, 144–156. https://doi.org/10.1016/j.foodhyd.2016.11.015

Phuhongsung, P., Zhang, M., & Bhandari, B. (2020). 4D printing of products based on soy protein isolate via microwave heating for flavor development. *Food Research International*, *137*, 109605. https://doi.org/10.1016/j.foodres.2020.109605

Ran, X., & Yang, H. (2022). Promoted strain-hardening and crystallinity of a soy protein-konjac glucomannan complex gel by konjac glucomannan. *Food Hydrocolloids*, *133*, 107959. https://doi.org/10.1016/j.foodhyd.2022.107959

Souza, C. J. F., & Garcia-Rojas, E. E. (2015). Effects of salt and protein concentrations on the association and dissociation of ovalbumin-pectin complexes. *Food Hydrocolloids*, *47*, 124–129. https://doi.org/10.1016/j.foodhyd.2015.01.010

Tan, J., & Kerr, W. L. (2015). Rheological properties and microstructure of tomato puree subject to continuous high pressure homogenization. *Journal of Food Engineering*, *166*, 45–54. https://doi.org/10.1016/j.jfoodeng.2015.05.025

Van Buggenhout, S., Wallecan, J., Christiaens, S., Debon, S. J. J., Desmet, C., Van Loey, A., Hendrickx, M., & Mazoyer, J. (2015). Influence of high-pressure homogenization on functional properties of orange pulp. *Innovative Food Science & Emerging Technologies*, *30*, 51–60. https://doi.org/10.1016/j.ifset.2015.05.004

Varela, P., Pintor, A., & Fiszman, S. (2014). How hydrocolloids affect the temporal oral perception of ice cream. *Food Hydrocolloids*, *36*, 220–228. https://doi.org/10.1016/j.foodhyd.2013.10.005

Villay, A., Filippis, F. L. D., Picton, L., Le Cerf, D., Vial, C., & Michaud, P. (2012). Comparison of polysaccharide degradations by dynamic high-pressure homogenization. *Food Hydrocolloids*, *27*(2), 278–286. https://doi.org/10.1016/j.foodhyd.2011.10.003

Wang, F., Lyu, J., Xie, J., & Bi, J. (2023). Texture formation of dehydrated yellow peach slices pretreated by osmotic dehydration with different sugars via cell wall pectin polymers modification. *Food Hydrocolloids*, *134*, 108080. https://doi.org/10.1016/j.foodhyd.2022.108080

Wang, L., Zhang, M., Bhandari, B., & Gao, Z. (2016). Effects of malondialdehyde-induced protein modification on water functionality and physicochemical state of fish myofibrillar protein gel. *Food Research International*, *86*, 131–139. https://doi.org/10.1016/j.foodres.2016.06.007

Wang, W., Shen, M., Jiang, L., Song, Q., Liu, S., & Xie, J. (2020). Influence of *Mesona blumes* polysaccharide on the gel properties and microstructure of acid-induced soy protein isolate gels. *Food Chemistry*, *313*, 126125. https://doi.org/10.1016/j.foodchem.2019.126125

Wang, W., Shen, M., Liu, S., Jiang, L., Song, Q., & Xie, J. (2018). Gel properties and interactions of *Mesona blumes* polysaccharide-soy protein isolates mixed gel: The effect of salt addition. *Carbohydrate Polymers*, *192*, 193–201. https://doi.org/10.1016/j.carbpol.2018.03.064

Xia, M., Chen, Y., Guo, J., Huang, H., Wang, L., Wu, W., Xiong, G., & Sun, W. (2019). Water distribution and textual properties of heat-induced pork myofibrillar protein gel as affected by sarcoplasmic protein. *LWT—Food Science and Technology*, *103*, 308–315. https://doi.org/10.1016/j.lwt.2019.01.009

Yi, J., Gan, C., Wen, Z., Fan, Y., & Wu, X. (2021). Development of pea protein and high methoxyl pectin colloidal particles stabilized high internal phase Pickering emulsions for β-carotene protection and delivery. *Food Hydrocolloids*, *113*, 106497. https://doi.org/10.1016/j.foodhyd.2020.106497

Zhang, H.-H., Huang, G.-Q., Geng, X., Teng, J., & Xiao, J.-X. (2021). Interaction between ovalbumin and pectin and coacervate characterization. *Colloid and Polymer Science*, *299*(6), 943–953. https://doi.org/10.1007/s00396-021-04818-5

Zhao, X., Yang, Z., Gai, G., & Yang, Y. (2009). Effect of superfine grinding on properties of ginger powder. *Journal of Food Engineering*, *91*(2), 217–222. https://doi.org/10.1016/j.jfoodeng.2008.08.024

Zhuang, X., Han, M., Jiang, X., Bai, Y., Zhou, H., Li, C., Xu, X.-L., & Zhou, G.-H. (2019). The effects of insoluble dietary fiber on myofibrillar protein gelation: Microstructure and molecular conformations. *Food Chemistry*, *275*, 770–777. https://doi.org/10.1016/j.foodchem.2018.09.141

SUPPORTING INFORMATION

Additional supporting information can be found online in the Supporting Information section at the end of this article.

How to cite this article: Xie, J., Lyu, J., Wang, F., Bai, L., & Bi, J. (2024). Characterization of fruit pulp-soy protein isolate (SPI) complexes: Effect of superfine grinding. *Journal of Food Science*, 1–16. https://doi.org/10.1111/1750-3841.16911